Accepted to ApJ
Preprint typeset using LaTeX style emulateapj v. 03/07/07

GRB 090902B: AFTERGLOW OBSERVATIONS AND IMPLICATIONS

S. B. Pandey[1,2], C. A. Swenson[3], D. A. Perley[4], C. Guidorzi[5], K. Wiersema[6], D. Malesani[7], C. Akerlof[1], M. C. B. Ashley[8], D. Bersier[9], Z. Cano[9], A. Gomboc[10], I. Ilyin[11], P. Jakobsson[12], I. K. W. Kleiser[4], S. Kobayashi[9], C. Kouveliotou[13], A. J. Levan[14], T. A. McKay[1], A. Melandri[9], C. J. Mottram[9], C. G. Mundell[9], P. T. O'Brien[6], A. Phillips[8], J. M. Rex[4], M. H. Siegel[9], R. J. Smith[9], I. A. Steele[9], G. Stratta[15], N. R. Tanvir[6], D. Weights[16], S. A. Yost[17], F. Yuan[1], W. Zheng[1]

Accepted to ApJ

ABSTRACT

The optical-infrared afterglow of the LAT-detected long duration burst, GRB 090902B, has been observed by several instruments. The earliest detection by ROTSE-IIIa occurred 80 minutes after detection by the GBM instrument onboard the *Fermi* Gamma-Ray Space Telescope, revealing a bright afterglow and a decay slope suggestive of a reverse shock origin. Subsequent optical-IR observations followed the light curve for 6.5 days. The temporal and spectral behavior at optical-infrared frequencies is consistent with synchrotron fireball model predictions; the cooling break lies between optical and XRT frequencies ~ 1.9 days after the burst. The inferred electron energy index is $p = 1.8 \pm 0.2$, which would however imply an X-ray decay slope flatter than observed. The XRT and LAT data have similar spectral indices and the observed steeper value of the LAT temporal index is marginally consistent with the predicted temporal decay in the radiative regime of the forward shock model. Absence of a jet break during the first 6 days implies a collimation-corrected γ-ray energy $E_\gamma > 2.2 \times 10^{52}$ ergs, one of the highest ever seen in a long-duration GRBs. More events combining GeV photon emission with multi-wavelength observations will be required to constrain the nature of the central engine powering these energetic explosions and to explore the correlations between energetic quanta and afterglow emission.

Subject headings: gamma rays: bursts

1. INTRODUCTION

The recently launched *Fermi* Gamma-Ray Space Telescope with the on-board Gamma-ray Burst Monitor (GBM) and Large Area Telescope (LAT) instruments (Atwood et al. 2009; Meegan et al. 2009) in conjunction with the *Swift* narrow field instruments (Gehrels et al. 2004) have opened a new window to understand the physical mechanisms that generate GeV photons in very energetic GRBs and the relation to lower energy components of the afterglow (Band et al. 2009). Since the *Fermi* launch more than a year ago, only 14 GRBs have been detected by the LAT while more than $\sim$ 350 bursts have been seen by the GBM during the same period. Optical afterglows have been detected for 7 of the 14 LAT events starting from $\sim$ 300 s to a few hours after the burst. The origin of these high-energy photons and their possible correlation to afterglow emission is still debated (Zou et al. 2009, and references therein). GRB 080916C (Abdo et al. 2009b), GRB 090510 (Abdo et al. 2009c; De Pasquale et al. 2010) and GRB 090902B (Abdo et al. 2009a) are among the brightest LAT bursts indicating some signatures consistent with the synchrotron forward shock models (Kumar & Barniol Duran 2009a,b; Ghirlanda et al. 2010). However, in the case of GRB 090902B, the deviation of the burst spectrum from the Band function and the observed large amplitude variability at very short time-scales (Abdo et al. 2009a) does not support the afterglow origin of the LAT data. High energy photons from GRBs have previously been observed by the EGRET detector and has shown evidence for deviations from synchrotron models (Hurley et al. 1994; Gonzalez et al. 2003).

The bright GRB 090902B (trigger 273582310) was detected by the GBM on 2009 Sep 2nd at 11:05:08.31 UT with an initial error box radius of 2-3 degrees centered at R.A. = $17^h\ 38^m\ 26^s$, Dec. = $+26^\circ\ 30'$ and a burst duration of 21.9 s in the energy band 50 - 300 keV (Bissaldi & Connaughton 2009). The burst was one of the brightest at LAT energies with a power-

[1] Randall Laboratory of Physics, Univ. of Michigan, 450 Church Street, Ann Arbor, MI, 48109-1040, USA
[2] Aryabhatta Research Institute of Observational Sciences, Manora Peak, Nainital, India, 263129
[3] Pennsylvania State Univ., 525 Davey Lab, University Park, PA 16802, USA
[4] Dept. of Astronomy, Univ. of California, Berkeley, CA 94720-3411, USA
[5] Dipartimento di Fisica, Università di Ferrara, via Saragat 1, I-44100, Ferrara, Italy
[6] Dept. of Physics and Astronomy, Univ. of Leicester, University Road, Leicester, LE1 7RH, UK
[7] Dark Cosmology Centre, Niels Bohr Institute, Univ. of Copenhagen, Juliane Maries vej 30, DK-2100 Copenhagen Ø, Denmark
[8] School of Physics, Univ. of New South Wales, Sydney NSW 2052, Australia
[9] Astrophysics Research Institute, Liverpool JMU, Twelve Quays House, Egerton Wharf, Birkenhead, CH41 1LD, UK
[10] Faculty of Mathematics and Physics, Univ. of Ljubljana, Jadranska 19, SI-1000 Ljubljana, Slovenia
[11] Astrophysikalisches Institut Potsdam, An der Sternwarte 16, D-14482 Potsdam, Germany
[12] Centre for Astrophysics and Cosmology, Science Institute, Univ. of Iceland, Dunhagi 5, IS-107 Reykjavík, Iceland
[13] NASA, Marshall Space Flight Center, NSSTC, 320 Sparkman Drive, Huntsville, Alabama, 35805, USA
[14] Dept. of Physics, Univ. of Warwick, Coventry, CV4 7AL, UK
[15] ASI SDC, via Galileo Galilei, 00044 Frascati, Italy
[16] Dept. of physical sciences, Univ. of Hertfordshire, College Lane, Hatfield, AL10 9AB, UK
[17] Dept. of Physics, College of St. Benedict, Collegeville, MN 56321, USA

law spectral distribution at both low and high energies (de Palma et al. 2009). The detailed analysis of the LAT and GBM data has been presented in Abdo et al. (2009a). The observed features in the prompt burst spectrum have also shown evidence for an underlying photospheric thermal emission (Ryde et al. 2010). ToO observations with *Swift* started $\sim$ 12.5 hours after the GBM trigger. The X-ray afterglow was detected within the LAT error-circle by the XRT (Kennea & Stratta 2009), the UVOT (Swenson & Siegel 2009) and later by several other ground-based multiwavelength facilities. The burst redshift, $z = 1.822$, was determined by the Gemini-North telescope (Cucchiara et al. 2009). The afterglow was also seen at radio frequencies by the WSRT (van der Horst et al. 2009) and by the VLA (Chandra & Frail 2009).

The details of the optical-infrared (IR) observations along with the temporal and spectral properties of the afterglow are described in the next section. In §3, we discuss the observed properties of the afterglow and comparisons to various models. These results are summarized in §4. Throughout the paper, we use the usual power-law representation of flux density, $f_\nu(t) \propto \nu^{-\beta} t^{-\alpha}$, for the regions without spectral breaks where α and β are the power-law temporal decay and spectral indices, respectively. For the cosmological calculations we have used the cosmological parameters $H_0 = 71$ km s^{-1}Mpc^{-1}, $\Omega_M = 0.27$, $\Omega_\Lambda = 0.73$. Errors are quoted at the 1-sigma level unless otherwise stated.

2. OBSERVATIONS AND DATA REDUCTION

The receipt of a ground-corrected GBM trigger with a 1 degree nominal location error initiated an observing sequence for ROTSE-IIIa, located at the Siding Spring Observatory in Australia. The telescope began taking three sets of thirty 20-s images, tiled around the GBM estimated location. Only the third set, starting 80 minutes after the burst, with R.A. = $17^h\ 38^m\ 13^s$ and Dec. = $+27^\circ\ 30'\ 59''$, covered the XRT burst location later identified as R.A. = $17^h\ 39^m\ 45.26^s$ and Dec. = $+27^\circ\ 19'\ 28.1''$ (Kennea & Stratta 2009). A substantial fraction of the delay was imposed by the overlap of a previous observation request for an unrelated field. Since the burst occurred during the early afternoon in Namibia and Turkey, ROTSE-IIIc and d could not respond until 6 hours later at which point similar sequences of images were obtained. The raw images were processed using the standard ROTSE software pipeline and photometry was performed on co-added images using the method described in Quimby et al. (2006). The ROTSE-IIIa observations were taken under bright night sky conditions with a lunar phase two days short of full. By the time the relevant exposures began, the transient was 13 ° above the horizon, decreasing to less than 11 ° at completion.

Because of the difficult observing environment, we carefully examined various possibilities that could lead to a false identification. All such efforts were confined to a 329×304 pixel sub-image spanning $18'\times17'$, centered at the OT. Within this field, 34 false positives were identified by SExtractor with signatures similar to the GRB OT. After correcting for the small fraction of the image too bright for such detections, the probability of such an event within a 5×5 pixel region close to the GRB coordinates established by later observations is less than 1%.

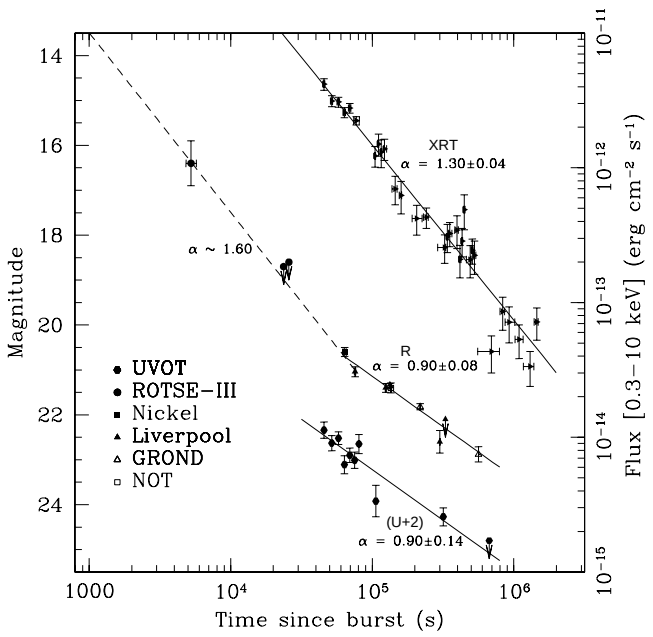

FIG. 1.— X-ray and optical afterglow light curves of the GRB 090902B. The solid lines mark the best fit power-laws to the XRT, u and R band light curves. An offset of 2 magnitudes has been applied to the $u-$band data for clarity. The power-law segment between the first ROTSE data point and the Nickel data is shown by a dashed line.

We next examined the sequence of 30 images carefully to determine if the apparent OT signal was an artifact of one or two frames with spurious problems. Five USNO stars with $13.2 \leq m_R \leq 14.3$ were chosen to establish the image point spread function and the sky extinction, frame-by-frame. Not surprisingly, the sky extinction and the ambient sky brightness increased by 30% and 20%, respectively, over the 890 second duration of these observations. For each image, the OT amplitude was determined and the entire set was fit to a power-law in time, constrained to the observation obtained by the Nickel telescope (Perley et al. 2009) 17 hours post-burst. The best fit corresponds to $m_R = 16.4\pm0.5$ at $t = 5320$ s after the burst and located within $1''$ of later, deeper detections. Based on the statistical analysis of the total ensemble of 30 measurements, we estimate a spurious detection probability of less than 1%. Combined with the spatial localization constraint, the probability of a false identification is less than 1×10^{-4}.

The UVOT magnitudes in u band were calculated using the UVOT photometric system (Poole et al. 2008) and the XRT data were reduced using the standard tools (Evans et al. 2001). The V, R and I magnitudes of the afterglow from the data taken by 1.0m Nickel, 2.0m Liverpool and 2.5m NOT telescopes were computed using nearby stars in the GRB field calibrated on October 10 under good photometric sky conditions by the 2.5m NOT telescope. The r' magnitudes were obtained using GROND (for details McBreen et al. 2010; Olivares et al. 2009). The J and K magnitudes of the afterglow were computed with respect to nearby 2MASS stars from the data taken by 3.8m UKIRT and 4.2m WHT. The photometry of the optical afterglow from these observations are summarized in Table 1 and the V, R, I magnitudes of the 5 nearby stars in the GRB field are given in Table 2.

Table 1. Observations of the afterglow of GRB 090902B at optical-IR frequencies by the consortium of telescopes.

Time since GRB (s)	Filter	Telescope	Exposure time (s)	Magnitude
4803	R	0.45m ROTSE-IIIa	890	16.4±0.5
23245	R	0.45m ROTSE-IIId	846	>18.7
25438	R	0.45m ROTSE-IIIc	892	>18.6
62291	R	1.0m Nickel	5×600+300	20.60±0.10
74749	R	2.0m Liverpool	2×900	21.04±0.11
123605	R	2.0m Liverpool	2×900	21.40±0.10
299554	R	2.0m Liverpool	2×900	22.60±0.25
328027	R	2.0m Liverpool	2×900	>22.1
153674	i'	2.0m Liverpool	2×900	21.33±0.15
330039	i'	2.0m Liverpool	2×900	>21.5
132935	r'_{AB}	2.2m GROND	738	21.54±0.05
218021	r'_{AB}	2.2m GROND	738	22.01±0.07
563787	r'_{AB}	2.2m GROND	738	23.07±0.17
135552	I	2.5m NOT	3×300	20.72±0.11
134499	R	2.5m NOT	3×300	21.40±0.11
133462	V	2.5m NOT	3×300	21.67±0.11
164490	J	3.8m *UKIRT-WFCAM*	1080	20.20±0.20
164780	K	3.8m *UKIRT-WFCAM*	1080	18.90±0.25
122083	J	4.2m *WHT-LIRIS*	24×75	19.99±0.15
125366	K	4.2m *WHT-LIRIS*	48×54	18.92±0.20
45097	u	*Swift*-UVOT	1075	20.34±0.18
50891	u	*Swift*-UVOT	1616	20.63±0.17
56674	u	*Swift*-UVOT	1997	20.52±0.14
62458	u	*Swift*-UVOT	2589	21.11±0.20
68244	u	*Swift*-UVOT	2515	20.90±0.16
73990	u	*Swift*-UVOT	2552	21.01±0.18
79775	u	*Swift*-UVOT	1311	20.65±0.21
104201	u	*Swift*-UVOT	3853	21.92±0.35
312211	u	*Swift*-UVOT	10549	22.27±0.20
664679	u	*Swift*-UVOT	9969	> 22.8

Table 2. The $(\alpha_{2000}, \delta_{2000})$ of the 5 stars near the afterglow position and their standard magnitudes in V, R and I photometric passbands.

ID	α_{2000} (h : m : s)	δ_{2000} (◦ : ′ : ″)	V (mag)	R (mag)	I (mag)
A	17 39 48.8	+27 19 57.0	18.98±0.02	18.38±0.01	17.92±0.01
B	17 39 44.8	+27 19 26.0	18.67±0.01	18.35±0.01	17.93±0.02
C	17 39 42.7	+27 19 13.9	17.76±0.01	17.34±0.01	16.99±0.01
D	17 39 47.6	+27 18 46.7	17.79±0.01	17.39±0.01	17.02±0.01
E	17 39 49.2	+27 18 53.6	18.84±0.01	18.57±0.02	18.14±0.02

2.1. *Afterglow Light Curves and Spectral Energy Distribution*

The optical data for the afterglow taken in R, r' and u filters along with the publicly available XRT data are plotted in Figure 1. Single power-law fits to the R and u band data > 12.5 hours post-burst have temporal decay indices of 0.90 ± 0.08 and 0.90 ± 0.14 respectively. To obtain continuity, the ROTSE optical data require a steeper decline at earlier times, with a temporal decay index ~ 1.6 or greater. The XRT light curve is characterized by a single power-law with a decay index of 1.30 ± 0.04, starting from 12.5 hours to 17 days after the burst.

The *Swift*-XRT time averaged spectrum (~ 12.5 to 413 hours post burst) has been analyzed using XSPEC with an absorbed power-law model and $z = 1.822$, inferring a spectral index $\beta_X = 0.9 \pm 0.1$ and a rest-frame column density $N_H^z = (1.8 \pm 0.3) \times 10^{22}$ cm^{-2} in addition to the Galactic column density $N_H^G = (3.8 \pm 0.3) \times 10^{20}$ cm^{-2} in the direction of the burst. The spectral analysis of the XRT data between ~ 12.5 and 20 hours post burst determines a power-law index of $\beta_X = 1.0 \pm 0.1$ (and $N_H^z = (2.4 \pm 0.4) \times 10^{22}$ cm^{-2}). For the period of ~ 20 to 413 hours, the comparable value is $\beta_X = 0.75 \pm 0.25$ (and $N_H^z = (0.7 \pm 0.4) \times 10^{22}$ cm^{-2}), indicating no significant spectral evolution during these observations. In subsequent analysis, a value of 0.9 ± 0.1 will be assumed for β_X. The afterglow spectral energy distribution (SED) is constructed at ~ 1.9 days post-burst using optical-IR data at K, J, I, r', R, V and u bands along with the XRT data as shown in Figure 2. The optical-IR spectral index, after correcting only for the Galactic extinction $E(B-V) = 0.04$ mag (Schlegel et al. 1998), has $\beta_O = 0.68 \pm 0.11$, flatter than that measured at XRT frequencies.

3. RESULTS AND DISCUSSIONS

3.1. *The Optical Brightness and LAT-Detected Bursts*

The power-law decays seen in other early optical afterglows of GRBs (Panaitescu & Vestrand 2008; Oates et al. 2009) suggest that the single observed data point at ~ 1.4 hours is unlikely to be a flaring feature at such late times. For an observation ~ 1.4 hours after the burst, the ROTSE detection at $m_R \sim 16.4$ mag is remarkably bright. This is best qualified by the statistical study of a large ensemble of bursts afterglows by Akerlof & Swan (2007). They found that the temporal evolution of the brightness distribution is well described by a power-law exponent, $\alpha \sim 0.7$. With that behavior, a magnitude of 16.4 at 1.4 hours would have evolved from $m_R \sim 15.2$ at t = 1000s and thus lie among the top 5 %

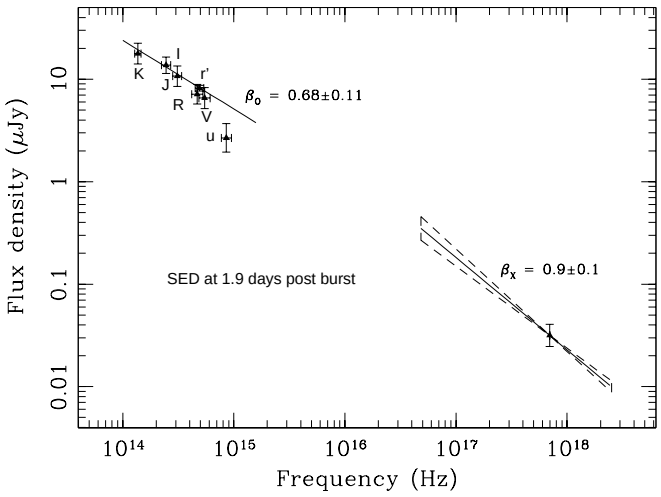

FIG. 2.— Multi-wavelength spectral energy distribution of the GRB 090902B afterglow at optical-IR and XRT frequencies derived at 1.9 days post-burst. The epoch has been chosen to allow the best possible spectral coverage. The observations in the u band might be effected by Ly-α and hence were excluded to determine the spectral index β_O.

of all bursts. Even one-magnitude errors in the ROTSE measurement would not substantially modify this conclusion. At later times, the optical afterglow must drop with a much steeper slope of > 1.6. If this behavior was manifested earlier, the brightness of GRB 090902B was even more pronounced.

The apparent temporal decay index, $\alpha > 1.6$, between 1.4 to 12.5 hours is steeper than the value of $\alpha = 0.90 \pm 0.08$ for epochs > 12.5 hours by more than 7-σ and is consistent with the dominance of reverse shock origin (Sari & Piran 1999a; Kobayashi 2000; Zhang, Kobayashi& Meśzaŕos 2003) as seen recently for the energetic 'naked eye' GRB 080319B, on similar time scales (e.g. Bloom et al. 2009; Pandey et al. 2009b).

Comparison of the observed apparent optical brightness of GRB 090902B at ~ 1.4 hours to a much larger sample of pre-*Swift* and *Swift* optical afterglows (See Figure 1 Kann et al. 2007) also indicates that the GRB 090902B was one of the brightest at such early epochs. A handful of other examples of long-duration GRBs, detected by LAT and with measured redshift values (GRB 080916C (Greiner et al. 2009); GRB 090323 (Updike et al. 2009); GRB 090328 (Oates 2009); GRB 090926 (Haislip et al. 2009) and GRB 091003 (Gronwall & Starling 2009) have been observed at optical frequencies starting ~ 16 to 26 hours post-burst. Comparison of the observed apparent optical brightness of the LAT-detected bursts 16-26 hours post-burst to the sample published in Kann et al. (2007) indicates that the optical brightness of LAT-detected GRBs are typical except GRB 090926 (Haislip et al. 2009) which was one of the brightest even at ~ 20.0 hours post-burst. Thus, the late time behavior of LAT-detected GRBs at optical frequencies is not unusual.

3.2. *Afterglow Models and GRB 090902B*

The derived values of temporal and spectral indices from multi-wavelength data can be compared with the closure relations (Price et al. 2002) to discriminate between interstellar medium (ISM) and wind ambient profiles (Sari, Piran & Narayan 1998; Chevalier & Li 2000) and to infer the location of the cooling break, ν_c. For the observed values of α (> 12.5 hours) and β_O at optical frequencies, the closure relation $\alpha = 3\beta/2$ is satisfied within errors in case of the ISM model (Price et al. 2002) for the observed frequencies $\nu < \nu_c$. Also, the value of the temporal decay index at XRT frequencies is steeper than for the optical, which clearly rules out the wind model and requires the ISM model with ν_c between optical and XRT frequencies. The location of ν_c below XRT frequencies implies that the electron energy index is $p = 1.8 \pm 0.2$, deduced solely using the value of β_X. The value of p and the determined temporal slopes at optical frequencies are also consistent with the closure relation $\alpha = 3(p-1)/4$ within errors, valid for the spectral regime $\nu_m < \nu < \nu_c$ in case of the ISM model. However, the observed temporal decay index at XRT frequencies is inconsistent with the ISM model closure relation $\alpha = (3p-2)/4$ (for $\nu > \nu_c$) by 2.8σ and requires a steeper value of p than estimated. The predicted value of p for $\nu > \nu_c$ is 2.4±0.05 using the XRT temporal decay index $\alpha = 1.30 \pm 0.04$. The afterglow properties favor an evolution of ν_c between the XRT and optical frequencies during the observations with an expected β_O of 0.4 ± 0.1 for $p = 1.8 \pm 0.2$. The relatively shallower value of β_O than observed can be attributed to a moderate amount of extinction $A_V = 0.20 \pm 0.06$ mag for SMC-like dust and assuming $\leq 20\%$ of the u flux is affected by Ly-α at the SED epoch using the method described in Perley et al. (2008). The present optical-IR and XRT data have determined the value of ν_c that is contrary to the assumption of (Kumar & Barniol Duran 2009b) that ν_c lies above the XRT frequencies and thus implies a steeper value of p.

In the light of above discussions, the published radio data at 4.8 GHz (van der Horst et al. 2009) and 8.46 GHz (Chandra & Frail 2009) of GRB 090902B near the SED epoch was used to constrain location of the self absorption frequency ν_a. The expected value of the spectral index between 4.8 and 8.46 GHz will be $\sim$ -0.4, closer to the expected $\nu^{-1/3}$ spectral regime for $\nu_a < \nu_m$ in the case of slow-cooling forward shock model (Sari, Piran & Narayan 1998). The effect of scintillation has not been taken into account which might modify the flux values for the observed frequencies at early epochs. Using the observed flux values at the radio frequencies and assuming ν_m to be $< 5.0 \times 10^{14}$ Hz at $\sim 10^4$ s after the burst, the estimated value of the peak synchrotron flux at the SED epoch is ~ 0.5 milliJy. The values of the peak synchrotron flux and ν_m at the epoch of SED are used to constrain the value of ν_a using equation 4.9 of Sari & Esin (2001). The calculated value of $\nu_a < 10^8$ Hz is below the observed radio frequencies and in agreement with the slow-cooling model for $\nu_a < \nu_m$ at the epoch of the SED.

The analysis also indicates no signature of a possible jet-break before or during the period of our afterglow observations. For the measured fluence between 10 keV and 10 GeV (Abdo et al. 2009a), the inferred value

of the isotropic equivalent energy is $E_\gamma^{iso} = 3.6 \times 10^{54}$ ergs assuming a gamma-ray efficiency $\eta_\gamma = 0.2$ and the circumburst density $n = 1$ cm^{-3} (Frail et al. 2001). Based on the observed properties of the burst, if we limit the jet-break time to be greater than 6 days after the burst, the value of the jet opening angle is $\theta_j > 0.11$ rad which gives the collimation corrected energy $E_\gamma > 2.2 \times 10^{52}$ ergs, one of the highest ever inferred (Cenko et al. 2010). With known values of p, the measured XRT flux at 1 day after the burst and using the description given in Freedman & Waxman (2001), the isotropic fireball energy carried by electrons is $\epsilon_e E = 3.1 \times 10^{54}$ ergs, where ϵ_e is the fraction of shock energy carried by relativistic electrons, comparable to E_γ^{iso} (see also Starling et al. 2009; Tanvir et al. 2009). The constraint on the energetics of the burst is comparable to the energy budget in the case of magnetars (Usov V. V. 1992; Starling et al. 2009; Cenko et al. 2010) and could also be accommodated within the "collapsar" origin of GRBs (MacFadyen & Woosley 1999). The energy estimates of more LAT-detected GRBs in the future will help towards a better understanding the nature of the central engine powering these energetic events.

3.3. *Onset of the GeV Afterglow*

The detection of many delayed photons at energies > 1 GeV, the observed high value of the isotropic γ-ray energy and the very early peak time seen in the LAT light curve constrain the value of the bulk Lorentz factor Γ to be ~ 1000 (Abdo et al. 2009a). Such high values of Γ have also been estimated in the case of other LAT bursts, GRB 080916C (Abdo et al. 2009b; Greiner et al. 2009) and GRB 090510 (Abdo et al. 2009c; Ghirlanda et al. 2010). Along with the afterglow properties discussed in the previous sections, the very high value of Γ and the very early peak in the LAT light curve provide a good opportunity to test the LAT temporal decay and spectral properties (Abdo et al. 2009a) for an early onset of the afterglow in terms of synchrotron shock models (Sari, Piran & Narayan 1998; Sari & Piran 1999b).

Under the synchrotron fireball model, a power-law distribution can be assumed in both time and spectral domains. Based on the discussions in the previous section and assuming $\nu_c \sim 2 \times 10^{16}$ Hz at the epoch of SED, the extrapolated values of ν_m and ν_c at 100.0 s are $< 5.0 \times 10^{17}$ Hz and $\sim 8 \times 10^{17}$ Hz respectively (assuming a temporal scaling of $\nu_c \propto t^{-1/2}$ and $\nu_m \propto t^{-3/2}$), both below 10 keV. At the SED epoch, the observed flux density of 0.03±0.01 μJy (at 2.88 keV) will give rise to an extrapolated flux density of 450±150 μJy at 100.0 s assuming the temporal decay of ~ 1.3. The 1 GeV flux density calculated at 100.0 s (Abdo et al. 2009a) is ~ 0.004 μJy. These flux densities at 1 GeV and 2.88 keV imply a spectral index of ~ 0.9 at 100.0 s, in agreement with the XRT spectral index at the epoch of SED and the LAT spectral index within 2-σ (Abdo et al. 2009a; Ghisellini et al. 2009). This indicates that for GRB 090902B, both XRT and LAT frequencies share the same spectral regime with ν_c below XRT frequencies under the synchrotron model, although the temporal index of ~ 1.5, observed at LAT frequencies is steeper than the XRT temporal decay index 1.3±0.04. However, our results show that around 100.0 s, $\nu_m < \nu_c$ and the observed temporal decay index at LAT frequencies is marginally consistent with the expected temporal decay index of (2 - 6p)/7 in the radiative case of the synchrotron model (Sari, Piran & Narayan 1998). Recently, based on the bolometric afterglow luminosity estimates for radiative fireballs, the expected temporal decay index $t^{10/7}$ for the LAT frequencies (Ghisellini et al. 2009) is also close to the observed LAT temporal index of ~ 1.5.

In the case of another LAT-detected GRB 080916C, the value of spectral index at LAT frequencies is 1.1 ± 0.1 (Ghisellini et al. 2009) and the value of GeV flux density at 100.0 s is ~ 0.006 μJy (Abdo et al. 2009b). Using the XRT data analysis published in (Greiner et al. 2009), the extrapolated value of 2.88 keV flux density at 100.0 s is 250±50 μJy. For GRB 080916C, the spectral index between 2.88 keV and 1 GeV at 100.0 s comes out to be ~ 0.9, close to the spectral index seen at the LAT frequencies (Ghisellini et al. 2009). This also indicates that ν_c is between XRT and LAT frequencies at 100.0 s within the assumptions of the afterglow model proposed by (Greiner et al. 2009). In the case of GRB 090510, the multi-wavelength SED at 100.0 s after the burst supports the afterglow origin of LAT data in terms of synchrotron forward shock model with a possible energy injection at optical and XRT frequencies (De Pasquale et al. 2010). The observed values of XRT flux for GRB 080916C, GRB 090510 and GRB 090902B are typical for other well observed Swift GRBs[1] (Zheng, Deng & Wang 2009) at similar time scales.

Based on above discussion, the evidence in favor of synchrotron forward shock model for the observed GeV emission for GRB 090902B, GRB 090510 and GRB 080916C is consistent with the predictions made by (Zou et al. 2009). However, the hard photon index at LAT frequencies and the evidence for reverse shock emission in early optical data cannot rule out the possibilities of synchrotron self-Compton emission at LAT frequencies (Wang Dai & Lu 2001) and the Klein-Nishina suppression of high energy electrons at early times (Wang et al. 2010). Such processes would require theoretical modeling which is beyond the scope of this paper.

4. SUMMARY

We present the observations of the afterglow of GRB 090902B at optical-IR frequencies carried out from 80 min to 6.5 days after the burst. The comparison of the optical afterglow of GRB 090902B to other bright pre-*Swift* and *Swift* burst indicates that the optical afterglow was bright at early epochs but decreased at times to a level typical of other bursts. The apparently steeper temporal decay of the early optical data can be explained in terms of reverse shock emission based on the estimated value of the early peak time provided by the reverse shock emission model (Zhang, Kobayashi& Meśzaŕos 2003). These inferred parameters are also in agreement with the very early onset of the afterglow seen at LAT frequencies (Abdo et al. 2009a). The temporal and spectral decay nature at optical-IR frequencies at later epochs favor synchrotron forward shock model although temporal decay at XRT frequencies requires a steeper electron energy index than the deduced value of $p = 1.8 \pm 0.2$ solely from the XRT spectral index and ν_c between optical and XRT

[1] http://www.swift.ac.uk/xrt_curves

frequencies. The radio afterglow data constrains self-absorption frequency $\nu_a < \nu_m$ which is lower than the observed radio frequencies at the SED epoch. The LAT and XRT data of GRB 090902B share similar spectral slopes at early epochs and indicate towards their common origin under the synchrotron forward shock model for the radiative fireballs. Also, the present analysis can not rule out the possible non-synchrotron origin for the emission at LAT frequencies. The estimated value of E_γ along with the required amount of host extinction is consistent with a massive star origin for the burst. However, the delayed GeV emission and the delayed onset are commonly observed properties of both long and short-duration GRBs detected by the LAT (Abdo et al. 2009a,b,c) in spite of differences in many observed properties including the proposed differences for their progenitors. More LAT-detected GRBs, especially seen by the BAT as well, and their early follow-up observations using ground-based robotic telescopes will shed light on the temporal properties of the afterglows and their possible correlation with the observed GeV emission. Finally, the most tantalizing aspect of these observations is the realization that a great deal more could be learned if accurate LAT localizations could be made available more promptly.

This research has made use of the data obtained through the High Energy Astrophysics Science Archive Research Center Online service, provided by the NASA/Goddard Space Flight Center. The ROTSE project is supported by the NASA grant NNX08AV63G and the NSF grant PHY-0801007. The authors associated with the WHT and the UKIRT acknowledge the Isaac Newton Group of Telescopes at La Palma and the Science and Technology Facilities Council of UK respectively. DARK is funded by DNRF. We also thank Gabor Furesz for his observations with the NOT.

REFERENCES

Abdo, A. A., et al., 2009a, ApJ, 706, L138
Abdo, A. A., et al., 2009b, Science, 323, 1688
Abdo, A. A., et al., 2009c, submitted to Nature, arXiv:0908.1832
Band, D., et al., 2009, ApJ, 701, 1673
Akerlof, C. W. & Swan, H. F., 2007, ApJ, 671, 1868
Atwood, W. B., et al., 2009, ApJ, 697, 1071
Bissaldi, E., & Connaughton, V. 2009, GCN Circ., 9866
Bloom, J. S., et al., 2009, ApJ, 691, 723
Cenko, S. B., et al., 2010, ApJ, 711, 641
Chandra, P., & Frail, D. A. 2009, GCN Circ., 9889
Chevalier, R. A. & Li, Z. -Y, 2000, ApJ, 520, L29
Cucchiara, A., Fox, D. B., et al. 2009, GCN Circ., 9873
de Palma, F., Bregeon, J., & Tajima, H. 2009, GCN Circ., 9867
De Pasquale, M. et al., 2010, ApJ, 709, 146
Evans, P. A. et al., 2007, A&A, 469, 379
Frail, D. A. et al., 2001, ApJ, 562, L55
Freedman, D. L. & Waxman, E., 2001, ApJ, 547, 922
Gehrels, N., et al., 2004, ApJ, 611, 1005
Ghirlanda, G., et al., 2010, A&A, 510, L7
Ghisellini, G., et al., 2010, MNRAS, 403, 926
Gonzalez, M. M., et al., 2003, Nature, 424, 749
Greiner, J. et al., 2009, A&A, 498, 89
Gronwall G. & Starling R. L. C., 2009, GCN Circ., 9987
Haislip, J., 2009, GCN Circ., 9937
Hurley, K., et al., 1994, Nature, 372, 652
Kann, D. A. et al., 2007, Submitted to ApJ, arXiv:0712.2186
Kennea, J., & Stratta, G. 2009, GCN Circ., 9868
Kobayashi, S., 2000, ApJ, 545, 807
Kumar, P., & Barniol Duran, R. 2009a, MNRAS, 400, L75
Kumar, P., & Barniol Duran, R. 2009b, Submitted to MNRAS, arXiv:0910.5726
MacFadyen, A. I., & Woosley, S. E., 1999, ApJ, 524, 262
McBreen, S., et al., 2010, In preperation
Meegan, C., et al., 2009, ApJ, 702, 791
Oates S. R., 2009, GCN Circ., 9048
Oates S. R. et al., 2009, MNRAS, 395, 490
Olivares, F., et al., 2009, GCN Circ., 9874
Panaitescu, A. & Vestrand, W. T., 2008, MNRAS, 387, 497
Pandey, S. B., Zheng, W., et al., 2009a, GCN Circ., 9878
Pandey, S. B., et al. 2009b, A&A, 504, 45
Perley, D. A., Li, W., & Chornock, R. et al., 2008, ApJ, 688, 470
Perley, D. A., Kleiser, I. K. W., & Rex, J. M. 2009, GCN Circ., 9870
Poole G. et al. 2008, MNRAS, 383, 627
Price, P. A., Berger, E., Reichart, D. E., et al. 2002, ApJ, 572, L51
Quimby, R. M., et al. 2006, ApJ, 640, 402
Ryde, F., Axelsson E., Zhang, B. B., et al. 2010, ApJ, 709, L172
Sari, R. & Esin, A. A., 2001, ApJ, 548, 787
Sari, R. & Piran, T., 1999, ApJ, 517, L109
Sari, R. & Piran, T., 1999, ApJ, 520, 641
Sari, R., Piran, T. & Narayan R., 1998, ApJ, 497, L17
Schlegel, D. J., Finkbeiner, D. P. & Davis, M. 1998, ApJ, 500, 525
Starling, R. L. C., et al., 2009, MNRAS, 400, 90
Swenson, C. A., & Siegel, M. H. 2009, GCN Circ., 9869
Tanvir, N. R., et al., 2009, Submitted to ApJ, arXiv:0812.1217
Updike, A. C., et al., 2009, GCN Circ., 9026
Usov, V. V., 1992, Nature, 357, 472
van der Horst, A. J., Kamble, A. P. et al., 2009, GCN Circ., 9883
Wang, X. Y., Dai, Z. G. & Lu, T., 2001, ApJ, 556, 1010
Wang, X. Y., et al., 2010, ApJ, 712, 1232
Zhang, B., Kobayashi S. & Meśzaŕos P., 2003, ApJ, 595, 950
Zheng, W. K., Deng J. S. & Wang J., 2009, RAA, 9, 1103
Zou, Y. C., et al., 2009, MNRAS, 396, 1163